



HAL
open science

From Compartmentalization of Bacteria within Inorganic Macrocellular Beads to the Assembly of Microbial Consortia

Armand Roucher, Mickaël Morvan, Deniz Pekin, Martin Depardieu, Jean-Luc Blin, Véronique Schmitt, Manfred Konrad, Jean-Christophe Baret, Renal Backov

► **To cite this version:**

Armand Roucher, Mickaël Morvan, Deniz Pekin, Martin Depardieu, Jean-Luc Blin, et al.. From Compartmentalization of Bacteria within Inorganic Macrocellular Beads to the Assembly of Microbial Consortia. *Advanced Biosystems*, 2018, 2 (3), pp.1700233(1-7). 10.1002/adbi.201700233 . hal-01709051

HAL Id: hal-01709051

<https://hal.science/hal-01709051>

Submitted on 15 May 2019

HAL is a multi-disciplinary open access archive for the deposit and dissemination of scientific research documents, whether they are published or not. The documents may come from teaching and research institutions in France or abroad, or from public or private research centers.

L'archive ouverte pluridisciplinaire **HAL**, est destinée au dépôt et à la diffusion de documents scientifiques de niveau recherche, publiés ou non, émanant des établissements d'enseignement et de recherche français ou étrangers, des laboratoires publics ou privés.

From Compartmentalization of Bacteria within Inorganic Macrocellular Beads to the Assembly of Microbial Consortia

Armand Roucher, Mickaël Morvan, Deniz Pekin, Martin Depardieu, Jean-Luc Blin, Véronique Schmitt, Manfred Konrad, Jean-Christophe Baret,* and Rénal Backov*

Microorganisms are highly efficient biocatalysts. Yet making use of their capabilities for chemical transformations requiring synergistic interactions between different microbes is challenging as the competition for resources might reduce the diversity and ultimately disrupt the synergies. Here, a new method is proposed for constructing microbial consortia for the integration of multistep transformations. Bacteria are successively grown and trapped within semipermeable inorganic foams produced as millimeter-sized beads. The beads function as efficient living biocatalysts is demonstrated. These living heterogeneous biocatalysts are manipulated to perform cycles of biochemical reactions and furthermore assembled to perform preprogrammed sequences of reactions. This new family of living advanced biocatalysts should find applications in a wide range of basic research and industrial systems where complex tasks have to be performed by controlled consortia of microorganisms.

Microorganisms play an essential role in the degradation and transformation of raw materials. These transformations maintain living cells in their out-of-equilibrium status^[1] and lead to products with added value.^[2–4] Exploiting these capacities of microorganisms for chemical transformations is an efficient concept that has been used for decades already in practical and industrial systems. However, setting up such processes becomes increasingly complex when several types

A. Roucher, M. Morvan, Dr. D. Pekin, Dr. M. Depardieu, Dr. V. Schmitt, Prof. J.-C. Baret, Prof. R. Backov
CRPP, UPR8641, CNRS
University of Bordeaux
115 Avenue du Dr. Schweitzer, 33600 Pessac, France
E-mail: jean-christophe.baret@u-bordeaux.fr; backov@crpp-bordeaux.cnrs.fr
Prof. J.-L. Blin
UMR CNRS 7565 SRSMC
Université de Lorraine
BP70239 54506 Vandoeuvre-les-Nancy cedex, France
Dr. M. Konrad
Max Planck Institute for Biophysical Chemistry
Am Fassberg 11, 37077 Goettingen, Germany

 The ORCID identification number(s) for the author(s) of this article can be found under <https://doi.org/10.1002/adbi.201700233>.

© 2018 The Authors. Published by WILEY-VCH Verlag GmbH & Co. KGaA, Weinheim. This is an open access article under the terms of the Creative Commons Attribution License, which permits use, distribution and reproduction in any medium, provided the original work is properly cited.

DOI: 10.1002/adbi.201700233

of microorganisms contribute to the transformation of interest or to cycles of transformation. Compartmentalization in microbeads provides means to miniaturize and integrate functions based on individual biochemical processes,^[5] and to protect microorganisms from the competition with other species in individual ecological niches.^[6–9] Immobilization of living organisms within porous media was previously demonstrated in various soft matter systems.^[10–20] However, the growth of bacterial colonies is hindered by the lack of free volume restricting efficient cell growth and proliferation. The benefit of the growth in confined space—compared to traditional bacterial growth in liquid or soft-agar media—cannot be fully

exploited, for example, through the control of quorum sensing in confinement.^[21–23] Here, we use a sol-gel process to confine bacteria while maintaining viability, proliferation and metabolic activity.^[24–27] In contrast to a recently reported approach in which a single matrix was used to integrate cascades,^[28] we show a modular assembly concept associating beads functionalized with different types of bacteria working in synergy and thereby creating versatile user-defined artificial microbial consortia.^[29] Our system is based on the integration of microorganisms in the beads which therefore provides means to produce the enzyme in situ as compared to other reported systems based on the encapsulation of purified enzymes in polymeric capsules.^[30,31]

We generate beads of Silica High Internal Phase Emulsion (Si(HIPE)) to irreversibly entrap the bacteria in beads surrounded by a semi-permeable silica-based membrane^[32–34] (Figure 1). The characteristic features of porosities overall length scales of both the beads and the surrounding shell as well as for the entrapment of bacteria are presented in Figures S1–S3 (Supporting Information).

In order to determine the efficiency and stability of the bacteria entrapped within the silica shell, Si(HIPE) beads with and without shell are placed into four wells of a microtiter plate containing culture medium. Each day, over a period of 6 d, a fraction of the medium is spread on an agar plate to determine whether or not bacteria leaked out of the beads (Figures S4 and S5, Supporting Information). After only 1 h of incubation, bacteria colonized the culture medium in the absence of the silica shell. On

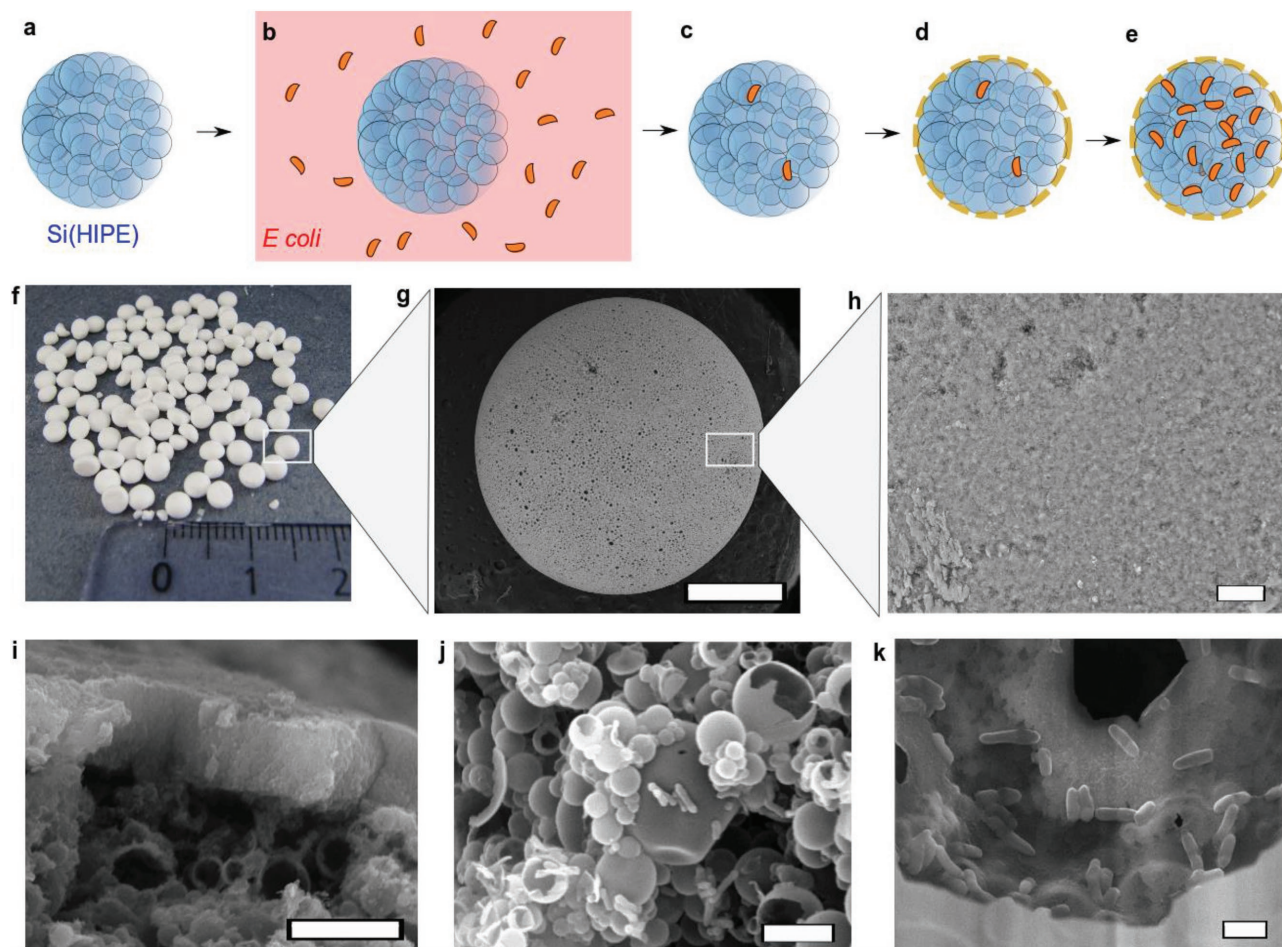


Figure 1. Production of bacteria-loaded Silica High Internal Phase Emulsion (Si(HIPE)). Si(HIPE) particles are produced as a) porous beads and b) imbibed with bacteria in culture medium. c) After inoculation of the bacteria (strain *E. coli* C41 (DE3) expressing *EcASNase-2*); d) a semipermeable SiO_2 -based layer is deposited on the surface; and e) bacteria are incubated for further proliferation inside the Si(HIPE). f) Photograph of the beads and details of the shell g) scale-bar 1 mm and h) scale-bar 20 μm showing the porous microstructure. i) Details of the membrane (scale-bar 10 μm). j) Scanning electron microscopy images of bacteria trapped within the bead after cultivation (scale-bar 5 μm); and k) zoom inside one pore (scale-bar 1 μm).

the contrary, after 1 h, 1 d, and 2 d, the four wells containing the beads with the silica shell still remain sterile (Figure S4, Supporting Information). The release of bacteria is only observed for one bead after 3 d whereas 75% of the wells remained sterile. After 6 d, 50% of the silica shell kept their impermeability. The protocol for the synthesis of the silica shell can certainly be improved to increase the resistance and the homogeneity of the bead coating, but our results show that the coating already has a half-life of about 6 d. Finally, we demonstrate that the suspension in contact with intact beads remains sterile. The beads are finally manually crushed and the suspension is then spread on Luria-Bertani (LB) agar plate (Figure S5, Supporting Information). The plates show a large amount of colonies demonstrating the bacteria viability after 6 d in the beads.

Bacterial metabolic activity is monitored by measuring the consumption of glucose delivered from the exterior of the compartment (Figure 2).

First, we perform the control glucose consumption assay for free *Escherichia coli* cells at different proliferation phases in bulk (Figure S6, Supporting Information; Figure 2f). For

$\text{OD}_{600 \text{ nm}} = 0.1$, 70% of glucose is consumed in 3 h, while the same consumption takes 6 h for bacterial colonies at $\text{OD}_{600 \text{ nm}} = 0.002$. The growth data are fitted with a model of growth providing a measurement of the doubling time of the bacteria, comparable to the expected value for *E. coli* in the medium (40–60 min, Figure S6, Supporting Information).

For the bacteria in the beads, we measure the glucose consumption in two steps (Figure 2g). First, two beads loaded with bacteria were incubated for 1 d in 2 mL of medium. At the end of the incubation, glucose is added to the medium to a concentration of $500 \times 10^{-6} \text{ M}$, and the concentration of glucose in the supernatant was measured over a period of 6 h after which the glucose consumption is complete, showing that the bacteria are metabolically active. The data are consistent with the model described by Equation S1 (Supporting Information). The proliferation time is found to be twice as long (1.25 h), and we estimate the population density as 2.5×10^6 bacteria per bead after 1 d of incubation. The beads are then re-suspended in culture medium for another day. Glucose is again added to the medium to $500 \times 10^{-6} \text{ M}$, and the glucose concentration is

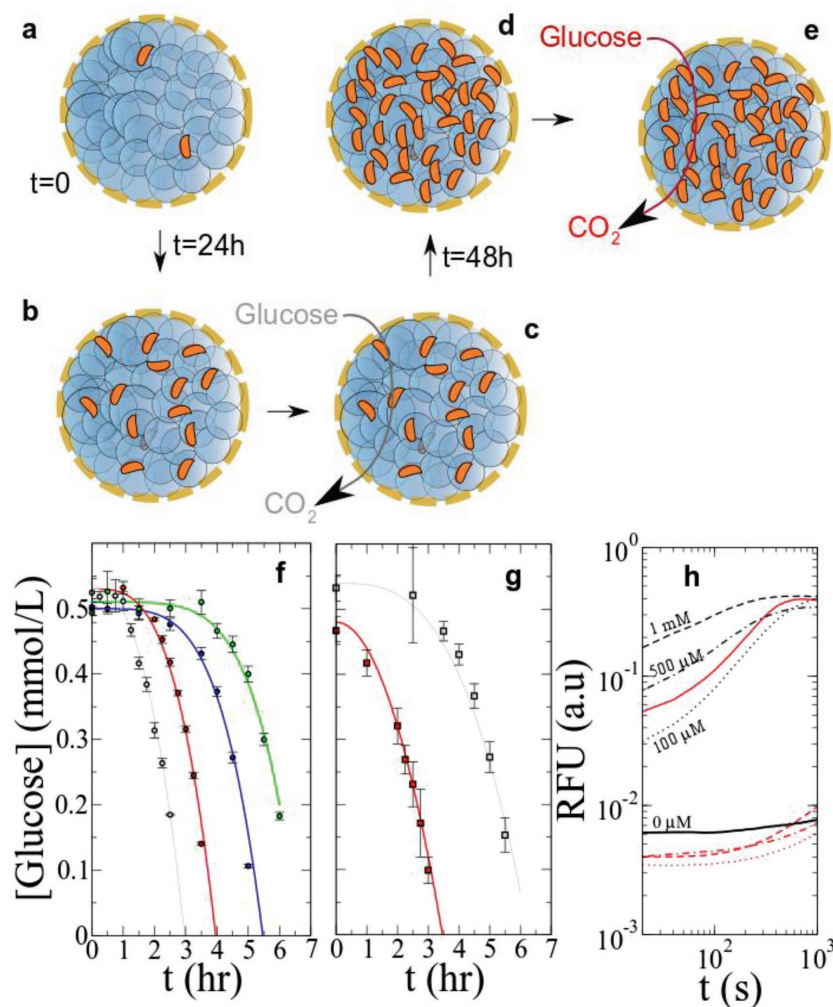


Figure 2. Glucose consumption in beads. a) Bacteria-expressing *L*-asparaginase EcASNase-2 uses the external medium to grow at $t=0$. b,c) After inoculation of the beads, culturing is performed for 1 d, and the glucose concentration in the medium is measured. d,e) The beads are then reincubated for 2 d, and the glucose assay is again performed. f) Glucose consumption by the free bacteria at $OD = 0.002$ (green), 0.01 (blue), 0.025 (red), 0.1 (gray) (Figure S4, Supporting Information). The time courses are fitted according to Equation 1 (Supporting Information) (Figure S5, Supporting Information). g) Glucose consumption by bacteria inside the beads after 1 d (b,c), white squares) and 48 h (d,e) red squares). h) The encapsulated bacteria are cultured for 1 d with 100×10^{-6} , 500×10^{-6} , 1×10^{-3} , or 2×10^{-3} M of glucose, to determine the amount of glucose used for bacterial growth. The residual glucose concentration is measured using the Amplex Red Glucose/Glucose Oxidase Assay Kit from Molecular Probes. For initial concentrations of glucose of 100×10^{-6} M (red dotted line), 500×10^{-6} M (red dashed line), and 1×10^{-3} M (red dotted and dashed line), the residual concentration is at the background level (full black line). For 2×10^{-3} M initial concentration (red full line), the residual concentration is of the order of $100\text{--}500 \times 10^{-6}$ M (black dotted line and dotted and dashed lines).

measured over time. After 3 h, all the glucose is consumed. The kinetics are consistent with Equation S1 (Supporting Information) with a similar proliferation time (1.3 h), but we reach a density of 10^7 bacteria per bead. During the 6 h of the first glucose consumption, the doubling time of the bacteria is 1.25 h corresponding to five doublings. The total number of cells in the bead would be at maximum ≈ 30 times larger than the initial cell number. At the start of the second glucose feeding, the number of cells is only four times larger than at the start of the

first glucose feed which indicates that a fraction of the cells may have died between the two glucose feeds, as is expected in standard cell culture. The volume of one single bead is of the order of $30 \mu\text{L}$. After 1 d of incubation, a single bead contains 2.5×10^6 cells, corresponding to a density of bacteria of $\approx 8 \times 10^7 \text{ cell mL}^{-1}$ ($OD_{600 \text{ nm}} \approx 0.8$), and after 48 h, the density reaches $OD_{600 \text{ nm}} \approx 3.2$. These results indicate that the density of cells in the beads is large providing extremely active microbial systems. For the sake of completeness, we estimate the glucose consumption for bacteria in capsules incubated at 37°C during day 1 (Figure 2h and Supporting Information) in the presence of increasing glucose concentrations ranging from 100×10^{-6} to 2×10^{-3} M. We observe that up to 2×10^{-3} M glucose, all the glucose is consumed, which is consistent with the data of Figure 2e. Our results show that glucose is effectively transported through the silica-based membrane, and that the activity of the bacteria inside the capsule is increasing over time as a result of proliferation.

We now demonstrate that our capsules are effective biocatalysts using a fluorogenic cascade of reactions applied to the measurement of *L*-asparaginase activity^[35] (Figure 3a,b). For free *E. coli* cells producing *L*-asparaginase, we observe an increase of the fluorescence corresponding to resorufin production followed by a decrease of fluorescence in the late phase of the kinetic assay as was already shown before resulting from production of resazurin from resorufin.^[36,37] The kinetics of the enzymatic reaction is measured as a function of the cell densities ranging from $OD_{600 \text{ nm}} = 0.00125$ to 0.1 to determine the maximum velocity of the reaction (Figure S8, Supporting Information). We then monitor the activity of bacteria trapped in the beads. As negative controls, we determine the *L*-asparaginase hydrolysis for the phosphate-buffered saline (PBS) and the beads free of bacteria. The inorganic capsule alone displays no hydrolysis reaction above the background. With the inorganic capsules, we obtain a fluorescence increase that is compared to that of the free bacteria. As in this case, the kinetics shows a distorted profile compared to the free bacteria, we focused on the initial rate (for times smaller than 500 s). Using the maximum velocity of the reaction in the beads (expressed in fluorescence units change per second), we find that the enzymatic activity of one single bead is equivalent to the activity of a bulk suspension at $OD_{600 \text{ nm}} \approx 0.01$ (inset of Figure 3b). For the bulk suspension at $OD_{600 \text{ nm}} = 0.01$, we have 2×10^5 bacteria in the $200 \mu\text{L}$ well. We therefore expect 2×10^5 cells per bead, corresponding to a cell density of $OD_{600 \text{ nm}} \approx 0.06$ for a bead of about $30 \mu\text{L}$. This cell

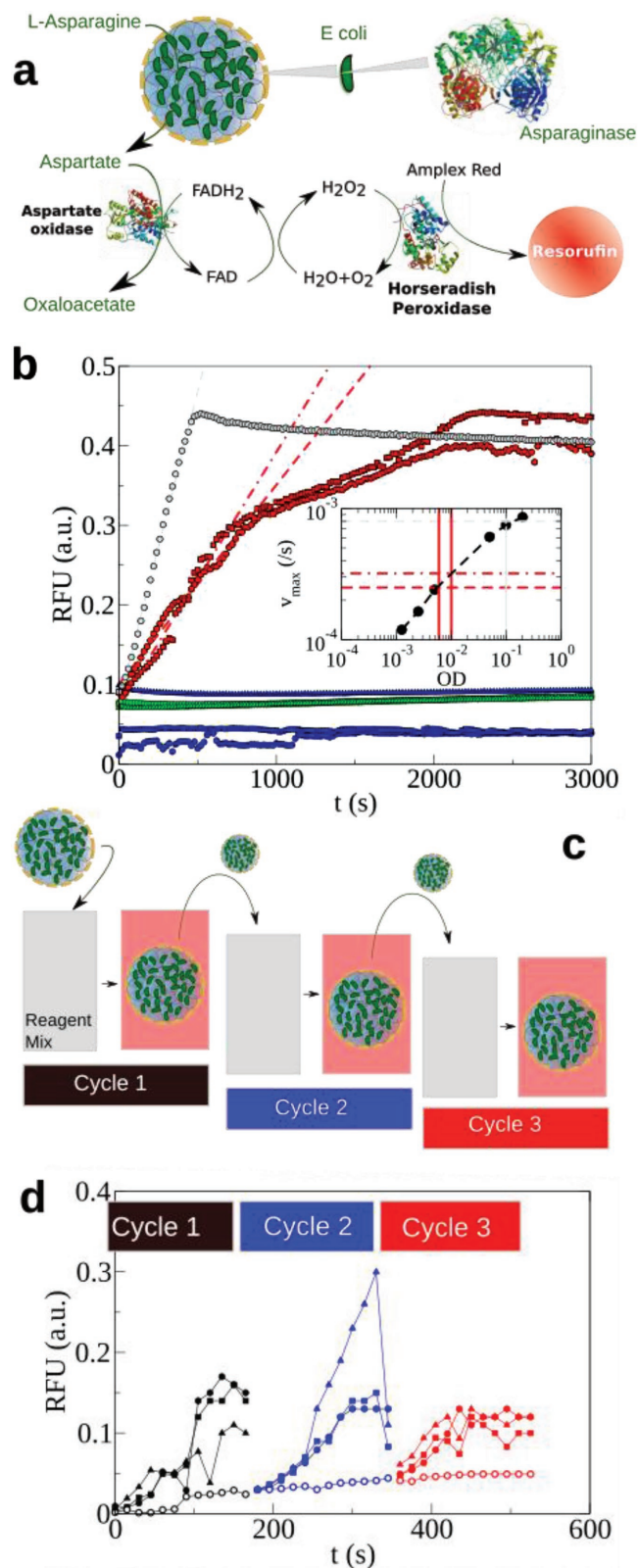


Figure 3. Integration of a complex reaction and recycling capabilities. a) The L-asparaginase activity of bacteria is assayed inside the beads. The reaction used for the detection of the enzymatic activity of L-asparaginase on its natural substrate involves a cascade of activities in the

density is very close to the density of cells used for the imbibition of the bead ($OD_{600\text{ nm}} = 0.1$), and therefore suggests that the bacteria freely diffuse through the beads during the imbibition, and that they are equilibrated in the beads at the same density as outside of the beads.

We point out that the cells do not proliferate to levels as high as when they are fed with glucose: as a reminder, the number of cells per beads in the case of the glucose experiment was 2×10^6 to 10^7 , while for the cells expressing L-asparaginase, we reached 2×10^5 cells per bead. The bacteria trapped inside the beads are therefore catalytically active, and all the constituents of the assay are free to permeate across the capsule membrane. A single capsule acts as a biocatalyst with an activity corresponding to hundreds of thousands of microorganisms. We then show that our capsules behave as heterogeneous catalysts displaying reusability and cycling capabilities. When the capsule is placed in fresh medium, the conversion of asparagine to aspartate restarted, and the process is repeated three times (Figure 3c,d). The slope of each curve at the initial time (expressed in fluorescence units per unit of time) of each cycle is almost constant for the three cycles ($6.1 \times 10^5 \text{ min}^{-1}$ for cycle 1, $5.8 \times 10^5 \text{ min}^{-1}$ for cycle 2, and $5.9 \times 10^5 \text{ min}^{-1}$ for cycle 3). As a note, the control experiments show a weak fluorescence increase, mainly due to spontaneous Amplex Red oxidation with time, the Amplex Red stock solution being prepared at the start of the first cycle.

From the measurements described above, we obtain a reproducible production of the beads and demonstrate possible reuse of the same bead. We further test the reproducibility of our approach by repeating the experiments on a larger cohort of twenty beads of varying sizes, starting from a fresh preparation of cells. We observe two sources of variability (Figure 4a).

The first source is mainly due to the expression level of the enzyme by our micro-organisms which varies from one experiment to the next. Here, the kinetics for free bacteria is four times slower than previously observed (Figure 2), probably related to a weaker expression of the enzyme. The kinetics in the beads is expected to follow the same trend.

We measure the asparaginase activity of bacteria inside the beads (Figure 4a). As mentioned before, for negative controls we monitor the L-asparagine hydrolysis for empty capsules surrounded by silica shell and for PBS. We group the beads in different size categories: small (size range from

surrounding medium catalyzed by a series of enzymes for coupling the reactions. b) The activity of a single bead is measured on duplicated experiments (red circles and squares) and compared to free bacteria at $OD_{600\text{ nm}} = 0.1$ (gray squares). Negative control includes PBS buffer (blue symbols) and an empty bead (green symbols). The different symbols correspond to replicated experiments. Inset: determination of the $OD_{600\text{ nm}}$ from the maximum velocity, based on the calibration provided in Figure S8 (Supporting Information). For free bacteria, the maximum velocity occurs at $OD_{600\text{ nm}} = 0.1$ as expected. For the beads, we obtain a corresponding $OD_{600\text{ nm}} = 0.01$. c) Principle of bead recycling. After a given reaction time, the reaction medium is replaced with fresh solution, and the capsules are reused for a second catalytic cascade. The process is repeated three times. d) Measurement of the cycling for three successive uses of the capsules. The different symbols correspond to replicates of the same experiments. Our experiments show the versatility of manipulation of our biocatalyst.

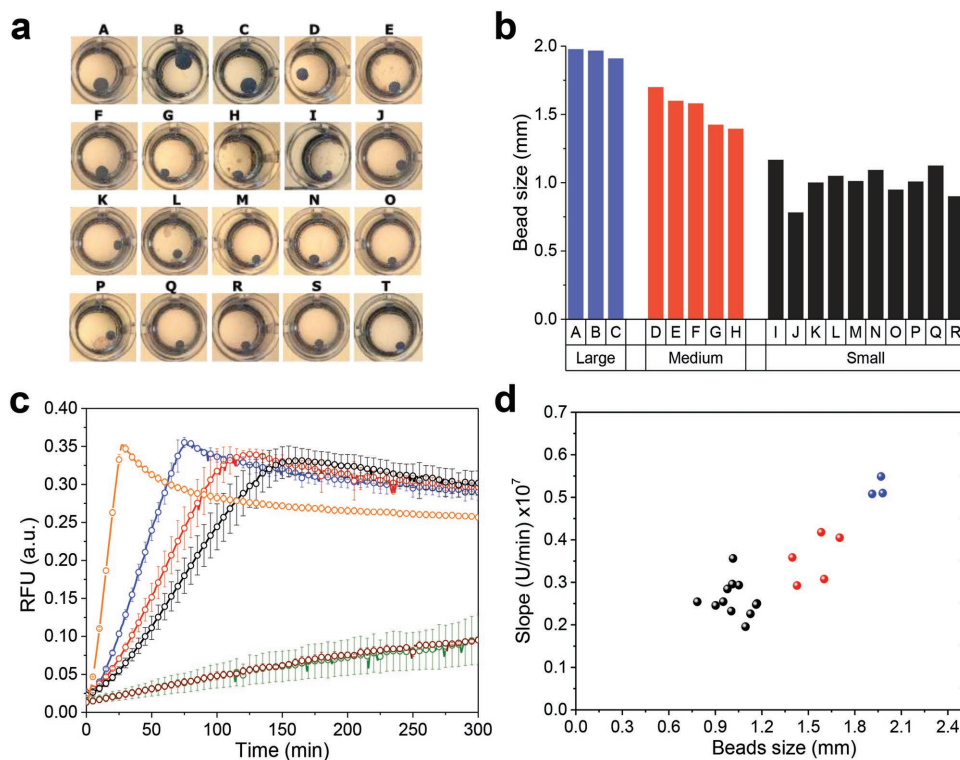


Figure 4. a) Photograph of the microplate containing the beads classified by size. b) Histogram of the beads size with three distinct populations. c) Activity of each beads population is measured (black curve for small size, red curve for medium size and blue curve for large size) and compared with bacteria suspension (orange curve). Negative control with PBS (brown curve) and empty beads (green curve). The curves presented are the average fluorescence of each population or triplicate experiment for suspension and negative control. d) Dependence of the maximum rate as a function of beads diameter.

0.7 to 1.2 mm), medium (ranging from 1.4 to 1.7 mm) and large beads with size close to 2 mm (Figure 4b). We obtain different kinetics all within the same order of magnitude, in qualitative agreement with the data of Figure 3 (Figure 4c). We determine the maximum speed of the reaction for the twenty beads and show that it correlates with the bead size (Figure 4d). The larger the size of the beads, the faster the kinetics as expected. Interestingly, the trend is close to linear as a function of size. In the case of a homogeneous and uniform distribution of cells in the beads, one would expect a cubic relationship (linear dependence in volume). Our results indicate that the active cells are likely to be located close to the surface; the structure of the bead should be taken into account to fully explain this linear relationship. Such a study is beyond the scope of the present manuscript, but we can draw an important conclusion: the kinetics of two small beads would be faster than that of a large bead of equivalent volume. This result is important for the further optimization of the bead production where smaller beads are preferable. Nevertheless, these measurements show that by controlling the size of the bead, we can control the hydrolysis rate.

The versatility of our approach is of interest for building up complex consortia of enzymes and cells acting in synergy. To demonstrate this idea, we reused the asparaginase assay, but produced two types of capsules. In one type, we grow asparaginase-expressing bacteria and in the second type of capsules we grow aspartate oxidase-expressing bacteria. Only in

the presence of both enzymes, the reaction cascade leading to fluorescence increase occurs (Figure 5a).

The catalytic activity of each capsule depends on the chemical reaction to be catalyzed by the bacterially expressed enzymes. Moreover, our capsules can be assembled with any user-defined stoichiometry to optimize the reaction kinetics in the cascade (Figure 5b–e). This point is relevant for the versatility of our micro-compartment system, since from analysis of free *E. coli* cells in suspensions we know that the ratio of the number of each type of bacteria determines the kinetics (inset of Figure 5f). We measure and compare the kinetics for bead stoichiometries ranging from 1:0 to 1:3. The cascade reaction becomes faster upon increasing the number of aspartate oxidase beads (Figure 5f), in qualitative agreement with the observation in bulk that the reaction is limited by the amount of aspartate oxidase.^[38] We note that the background increase observed in the case of beads containing only the asparaginase-overexpressing cells is likely to arise from the presence of aspartate oxidase endogenously expressed by our *E. coli* strains. This proof of concept result is of primary importance: it shows that the number and nature of the beads can be tuned according to the chemical kinetics or stoichiometry of the different reactions involved, thus offering a remarkable adaptability through this intrinsic modularity.

In summary, the capability to construct and assemble artificial microbiota or other cell consortia is of fundamental and practical interest. We demonstrate a modular design^[39] of solid

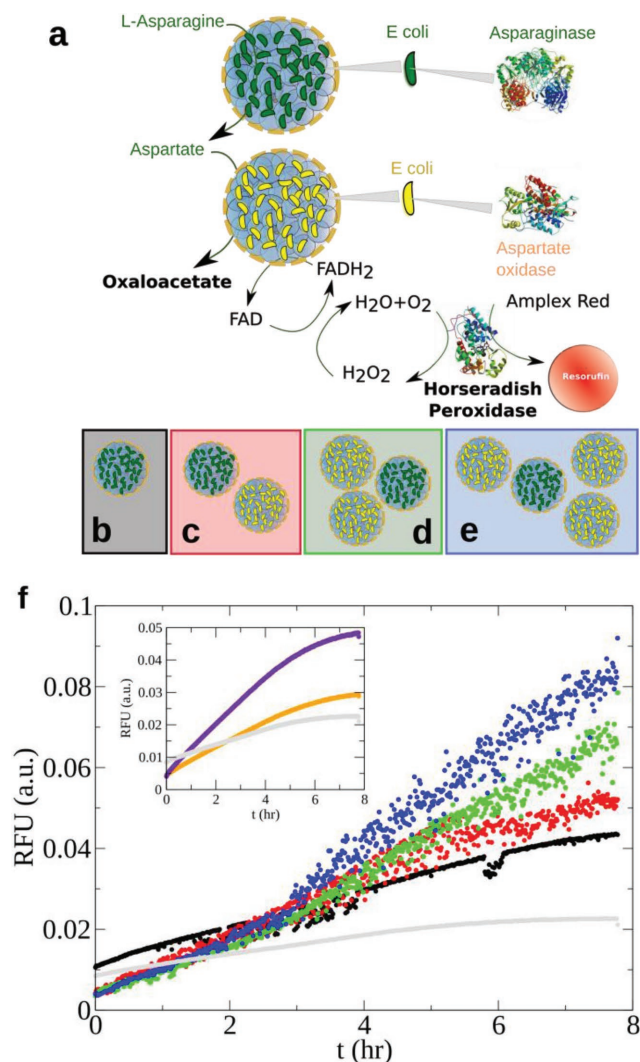


Figure 5. Integration of different types of beads for the construction of artificial cell consortia. a) Beads inoculated with bacteria expressing different enzymatic activities can be assembled to perform complex synergistic enzymatic cascades. Using the coupled-enzyme assay for detection of catalytic activity present in beads harboring *E. coli* cells (green) that express L-asparaginase, we now add to our system a second type of beads, loaded with *E. coli* cells (yellow) expressing aspartate oxidase. The fluorescent product Resorufin is generated only if either type of beads catalyzes the corresponding reaction. b–e) Several consortia are assembled and tested by varying the stoichiometry of the beads. Four cell consortia are tested. f) By increasing the number of aspartate oxidase beads, we enhance the kinetics of the reaction: (gray: control with no beads; black: background with no aspartate oxidase beads (b); red: consortium c; green: consortium d; blue: consortium e). Inset: control showing that aspartate oxidase is the limiting factor in the transformation using different optical densities of free cells. Bacteria overproducing asparaginase ($OD_{600\text{ nm}} = 0.1$) are mixed with cells expressing aspartate oxidase ($OD_{600\text{ nm}} = 0.1$ for the orange curve and $OD_{600\text{ nm}} = 1$ for the purple curve). The gray curve is the control with PBS buffer).

material-supported biocatalysts for the integration of cyclic processes and of complex cascade-type chemical reactions. Using the beads to perform a reaction in a batch reactor, no sterilization of the reactors is required once the beads are removed from the media. The reactions studied here are specific, dealing

with glucose oxidation, L-asparagine hydrolysis, and aspartate oxidation. Yet, the concept we designed for single and cascade-type reactions is generic and universal as long as the chemicals (substrates, intermediates, and products) involved in the enzyme-catalyzed reactions are able to diffuse through the porous structure holding the bacteria.

Our approach therefore provides a modular solution to the construction of complex microbial consortia with possible applications in the fields of chemistry for sequential heterogeneous catalysis, in the agro-industry for the transformation of biomass by micro-organisms, in energy production for hydrogen generation, in environmental science for nitrate reduction or CO_2 fixation processes, and in synthetic biology for the construction of mimics of specific microbiota.

Supporting Information

Supporting Information is available from the Wiley Online Library or from the author.

Acknowledgements

R.B. and J.-C.B. both acknowledge the support from the French Government “Investments for the Future” Programme, University of Bordeaux Initiative of Excellence (IDEX Bordeaux) (Reference Agence Nationale de la Recherche (ANR)-10-IDEX-03-02). J.-C.B. acknowledges support from European Research Council (ERC) Seventh Framework Programme (2007–2013) ERC Grant Agreement 306385–SOFT Interfaces and from the “Région Aquitaine”; R.B., J.-L.B and V.R. acknowledges support from the Agence Nationale de la Recherche, project ANR-Iseapim3. M.K. thanks the Max Planck Institute for Biophysical Chemistry for continuous funding. The technical support of Sébastien Gounel and Sabrina Bichon is warmly acknowledged.

Conflict of Interest

The authors declare no conflict of interest.

Keywords

biotechnology, catalysis, emulsion, foams, sol–gel

Received: November 28, 2017
Published online: January 22, 2018

- [1] E. Schroedinger, *What is Life? The Physical Aspect of the Living Cell*, Cambridge University Press, Cambridge, UK 1944.
- [2] I. H. Chapela, S. A. Rehner, T. R. Schultz, U. G. Mueller, *Science* **1994**, 266, 1691.
- [3] N. Amarger, *Biochimie* **2002**, 84, 1061.
- [4] J. Du, Z. Shao, H. Zhao, *J. Ind. Microbiol. Biotechnol.* **2011**, 38, 873.
- [5] R. J. Peters, M. Marguet, S. Marais, M. W. Fraaije, J. C. van Hest, S. Lecommandoux, *Angew. Chem., Int. Ed.* **2014**, 53, 146.
- [6] J. J. Walker, N. R. Pace, *Appl. Environ. Microbiol.* **2007**, 73, 3497.
- [7] R. U. Meckenstock, F. von Netzer, C. Stumpp, T. Lueders, A. M. Himmelberg, N. Hertkorn, P. Schmitt-Kopplin, M. Harir, R. Hosein, S. Haque, D. Schulze-Makuch, *Science* **2014**, 345, 673.

- [8] J. A. Mikucki, A. Pearson, D. T. Johnston, A. V. Turchyn, J. Farquhar, D. P. Schrag, A. D. Anbar, J. C. Prisco, P. A. Lee, *Science* **2009**, 324, 397.
- [9] A. S. Mao, J.-W. Shin, S. Utech, H. Wang, O. Uzun, W. Li, M. Cooper, Y. Hu, L. Zhang, D. A. Weitz, D. J. Mooney, *Nat. Mater.* **2017**, 16, 236.
- [10] D. Avnir, T. Coradin, O. Lev, J. Livage, *J. Mater. Chem.* **2006**, 16, 1013.
- [11] D. Fiedler, U. Hager, H. Franke, U. Soltmann, H. Boettcher, *J. Mater. Chem.* **2007**, 17, 261.
- [12] F. Lagarde, N. Jaffrezic-Renault, *Anal. Bioanal. Chem.* **2011**, 400, 947.
- [13] A. Leonard, P. Dandoy, E. Danloy, G. Leroux, C. F. Meunier, J. C. Rooke, B. Su, *Chem. Soc. Rev.* **2011**, 40, 860.
- [14] M. Blondeau, T. Coradin, *J. Mater. Chem.* **2012**, 22, 22335.
- [15] E. Michelini, A. Roda, *Anal. Bioanal. Chem.* **2012**, 402, 1785.
- [16] B. C. Kim, M. B. Gu, *Biosens. Bioelectron.* **2003**, 18, 1015.
- [17] J. R. Premkumar, E. Sagi, R. Rozen, S. Belkin, A. D. Modestov, O. Lev, *Chem. Mater.* **2002**, 14, 2676.
- [18] J. R. Premkumar, R. Rosen, S. Belkin, O. Lev, *Anal. Chim. Acta* **2002**, 462, 11.
- [19] K. Alessandri, K. Alessandria, B. R. Sarangi, V. V. Gurchenkov, B. Sinha, T. R. Kießling, L. Fetler, F. Rico, S. Scheuring, C. Lamaze, A. Simon, S. Geraldo, D. Vignjevi, H. Doméjean, L. Rolland, A. Funfak, J. Bibette, N. Bremond, P. Nassoy, *Proc. Natl. Acad. Sci. USA* **2013**, 110, 14843.
- [20] H. Domejean, H. Doméjean, M. de la Motte Saint Pierre, A. Funfak, N. Atrux-Tallau, K. Alessandri, P. Nassoy, J. Bibette, N. Bremond, *Lab Chip* **2017**, 17, 110.
- [21] J. Q. Boedicker, L. Li, T. R. Kline, R. F. Ismagilov, *Lab Chip* **2008**, 8, 1265.
- [22] J. C. Harper, S. M. Brozik, C. J. Brinker, B. Kaehr, *Anal. Chem.* **2012**, 84, 8985.
- [23] J. L. Connell, E. T. Ritschdorff, M. Whiteley, J. B. Shear, *Proc. Natl. Acad. Sci. USA* **2013**, 110, 18380.
- [24] A. Coiffier, T. Coradin, C. Roux, O. M. M. Bouvet, J. Livage, *J. Mater. Chem.* **2001**, 11, 2039.
- [25] N. Nassif, O. Bouvet, M. N. Rager, C. Roux, T. Coradin, J. Livage, *Nat. Mater.* **2002**, 1, 42.
- [26] N. Nassif, C. Roux, T. Coradin, M.-N. Rager, O. M. M. Bouvet, J. Livage, *J. Mater. Chem.* **2003**, 13, 203.
- [27] Z. Fazal, J. Pelowitz, P. E. Johnson, J. C. Harper, C. J. Brinker, E. Jakobsson, *ACS Nano* **2017**, 11, 3560.
- [28] B. R. Mutlu, J. K. Sakkos, S. Yeom, L. P. Wackett, A. Aksan, *Sci. Rep.* **2016**, 6, 27404.
- [29] K. Brenner, L. You, F. H. Arnold, *Trends Biotechnol.* **2008**, 26, 483.
- [30] J. Park, E. T. Hwang, B.-K. Seo, M. B. Gu, *ACS Catal.* **2016**, 6, 6175.
- [31] X. Wang, Z. Li, J. Shi, H. Wu, Z. Jiang, W. Zhang, X. Song, Q. Ai, *ACS Catal.* **2014**, 4, 962.
- [32] P. Hodge, D. C. Sherrington, *Polymer-Supported Reactions in Organic Synthesis*, Wiley, Chichester, UK **1980**.
- [33] F. Carn, A. Colin, M.-F. Achard, H. Deleuze, E. Sellier, M. Birotc, R. Backov, *J. Mater. Chem.* **2004**, 14, 1370.
- [34] M. Depardieu, M. Viaud, A. Buguin, J. Livage, C. Sanchez, R. Backov, *J. Mater. Chem. B* **2016**, 4, 2290.
- [35] J. Nomme, Y. Su, M. Konrad, A. Lavie, *Biochemistry* **2012**, 51, 6816.
- [36] V. Towne, M. Will, B. Oswald, Q. Zhao, *Anal. Biochem.* **2004**, 334, 290.
- [37] A. Zhu, R. Romero, H. R. Petty, *Anal. Biochem.* **2010**, 396, 146.
- [38] C. S. Karamitros, J. Lim, M. Konrad, *Anal. Biochem.* **2014**, 445, 20.
- [39] R. Backov, *Soft Matter* **2006**, 2, 452.